Palaeogeography, Palaeoclimatology, Palaeoecology 307 (2011) 301–312

Contents lists available at ScienceDirect

Palaeogeography, Palaeoclimatology, Palaeoecology

journal homepage: www.elsevier.com/locate/palaeo

Quantification of a greenhouse hydrologic cycle from equatorial to polar latitudes: The mid-Cretaceous water bearer revisited

Marina B. Suarez [a,*], Luis A. González [a], Gregory A. Ludvigson [b]

[a] Department of Geology, The University of Kansas, 1475 Jayhawk Blvd., Lindley Hall rm. 120, Lawrence, KS 66045 USA
[b] Kansas Geological Survey, 1930 Constant Ave., Lawrence, Kansas 66047 USA

ARTICLE INFO

Article history:
Received 5 August 2010
Received in revised form 4 May 2011
Accepted 16 May 2011
Available online 20 May 2011

Keywords:
Cretaceous
Paleoclimate
Pedogenic carbonates
Oxygen isotopes

ABSTRACT

This study aims to investigate the global hydrologic cycle during the mid-Cretaceous greenhouse by utilizing the oxygen isotopic composition of pedogenic carbonates (calcite and siderite) as proxies for the oxygen isotopic composition of precipitation. The data set builds on the Aptian–Albian sphaerosiderite $\delta^{18}O$ data set presented by Ufnar et al. (2002) by incorporating additional low latitude data including pedogenic and early meteoric diagenetic calcite $\delta^{18}O$. Ufnar et al. (2002) used the proxy data derived from the North American Cretaceous Western Interior Basin (KWIB) in a mass balance model to estimate precipitation–evaporation fluxes. We have revised this mass balance model to handle sphaerosiderite and calcite proxies, and to account for longitudinal travel by tropical air masses. We use empirical and general circulation model (GCM) temperature gradients for the mid-Cretaceous, and the empirically derived $\delta^{18}O$ composition of groundwater as constraints in our mass balance model. Precipitation flux, evaporation flux, relative humidity, seawater composition, and continental feedback are adjusted to generate model calculated groundwater $\delta^{18}O$ compositions (proxy for precipitation $\delta^{18}O$) that match the empirically-derived groundwater $\delta^{18}O$ compositions to within $\pm 0.5‰$. The model is calibrated against modern precipitation data sets.

Four different Cretaceous temperature estimates were used: the leaf physiognomy estimates of Wolfe and Upchurch (1987) and Spicer and Corfield (1992), the coolest and warmest Cretaceous estimates compiled by Barron (1983) and model outputs from the GENESIS-MOM GCM by Zhou et al. (2008). Precipitation and evaporation fluxes for all the Cretaceous temperature gradients utilized in the model are greater than modern precipitation and evaporation fluxes. Balancing the model also requires relative humidity in the subtropical dry belt to be significantly reduced. As expected calculated precipitation rates are all greater than modern precipitation rates. Calculated global average precipitation rates range from 371 mm/year to 1196 mm/year greater than modern precipitation rates. Model results support the hypothesis that increased rainout produces $\delta^{18}O$-depleted precipitation.

Sensitivity testing of the model indicates that the amount of water vapor in the air mass, and its origin and pathway, significantly affect the oxygen isotopic composition of precipitation. Precipitation $\delta^{18}O$ is also sensitive to seawater $\delta^{18}O$ and enriched tropical seawater was necessary to simulate proxy data (consistent with fossil and geologic evidence for a warmer and evaporatively enriched Tethys). Improved constraints in variables such as seawater $\delta^{18}O$ can help improve boundary conditions for mid-Cretaceous climate simulations.

1. Introduction

Water is a key factor in the evolution of life, biogeochemical cycles, and global temperature regulation and as such, an understanding of the hydrologic cycle and its changes over geologic time are important, especially in light of future climate change. Barron et al. (1989) posited that a warmer global climate should cause an intensification of the hydrologic cycle. Knowledge of the functioning of the hydrologic cycle under warmer and higher atmospheric CO_2 concentrations can be gained by the study of ancient greenhouse worlds. Given that current atmospheric pCO_2 already exceeds the range of pCO_2 values estimated for the more recent thermal maxima of the Pleistocene and Holocene (Soreghan et al., 2003; Ruddiman, 2005) study of much older systems with higher CO_2 concentrations are necessary to gain the much needed insights into potential high CO_2 scenarios. The mid-Cretaceous (Aptian–Albian) greenhouse world with its high pCO_2, shallow temperature gradients, warm high latitudes, absence of polar ice, and an intensified hydrologic cycle (Ludvigson et al., 1998; Jenkyns et al., 2004; Poulsen, 2004; Ufnar et al., 2004a, 2004b, 2004c) have the extreme conditions needed to help us ascertain the impact of increased atmospheric CO_2 concentrations.

* Corresponding author at: Department of Earth and Planetary Science, Johns Hopkins University, 3400 N. Charles St., 301 Olin Hall, Baltimore, MD 21218 USA.
E-mail address: msuarez5@jhu.edu (M.B. Suarez).

0031-0182/$ – see front matter © 2011 Elsevier B.V. All rights reserved.
doi:10.1016/j.palaeo.2011.05.027

Our knowledge of the mid-Cretaceous greenhouse world and particularly the hydrologic cycle response to increased global warmth has seen significant advances over the past two decades (Barron et al., 1989; Ludvigson et al., 1998; Hay and DeConto, 1999; White et al., 2001; Ufnar et al., 2002, 2004a; Poulsen et al., 2007; Suarez et al., 2009). This improved knowledge has led to the recognition that there are significant differences between climate model outputs and data inferred or extrapolated from geological and paleontological data. An important goal of recent studies has been to reconcile the known differences between climate models and climate proxies (e.g. Poulsen et al., 2007; Zhou et al., 2008), and to generate large proxy data sets and derived climate data (e.g. White et al., 2001; Sorensen, 2002; Ufnar et al., 2002, 2004a, 2004b, 2004c; Ludvigson et al., 2004). All of the research to date suggests some degree of intensified evaporation and precipitation during the mid-Cretaceous.

Ufnar et al. (2002) utilized Stella® Systems Modeling software to develop an oxygen isotope mass balance model to estimate the precipitation and evaporation fluxes needed to reproduce the observed $\delta^{18}O$ values of pedogenic sphaerosiderites collected from wetland paleosols between 35°N and 75°N paleolatitude. The sphaerosiderite $\delta^{18}O$ data exhibits a pronounced depletion at high latitudes and model results suggest that this depletion requires overall increases in precipitation. Increases in precipitation are particularly high in the mid to high latitudes. For example, at 45°N paleolatitude, the mass balance model indicates precipitation rates of 2618 mm/year, which is more than three times the modern precipitation rate (Ufnar et al., 2002, Table 3). While the Ufnar et al. (2002) model lacked the complexity of a general circulation model (GCM), its importance resides in the ability to utilize empirical data to quantify the hydrologic cycle as well as to provide new insights for improving the more complex GCMs as has been demonstrated by Poulsen et al. (2007).

An obvious limitation of the Ufnar et al. (2002) model is that the data used to constrain precipitation and evaporation fluxes were limited to mid to high latitudes. The goal of this study is to incorporate new data from sub-tropical and equatorial localities (SW U.S.A., Mexico, and Colombia) to improve constraints on the mass balance model. To do so, the proxy data set is expanded to include isotope data from pedogenic calcites found in more evaporative settings as well as sphaerosiderite data from near equatorial settings. In addition to the expanded isotope constraints, the model has been modified to include adjustable air mass origin and adjustable air mass pathways (particularly along longitude in the subtropics), as well as variable $\delta^{18}O$ of seawater and continental feedback.

2. Methods

2.1. Proxy data

The premise of using pedogenic carbonates as a proxy for the oxygen isotopic composition of precipitation stems from the recognition that in carbonate depositional systems, exposure surface interaction with meteoric water often results in calcite with narrow $\delta^{18}O$ compositions that reflect the oxygen isotopic composition of meteoric water (Allan and Matthews, 1977; Lohmann, 1988). Variable $\delta^{13}C$ compositions are the result of the original parent rock carbon compositions and soil CO_2 compositions (Allen and Matthews, 1977; Lohmann, 1988). Plotting these values in $\delta^{18}O$ vs. $\delta^{13}C$ space defines vertical trends called meteoric calcite lines (MCLs) (Lohmann, 1988), which were also recognized in pedogenic sphaerosiderites by Ludvigson et al. (1998) and termed meteoric sphaerosiderite lines (MSLs).

The majority of the data comes from American northern hemisphere localities. Mid to high latitude data was presented by White et al. (2001) and Ufnar et al. (2002) and consists of sphaerosiderite data from Aptian–Albian wetland or seasonally saturated soils from the Dakota Formation of Iowa, Nebraska, Kansas, and Utah, U.S.A.; the Swan River Formation of Manitoba and Saskatchewan, Canada (Ufnar et al., 2004b); the Mattagami Formation of Ontario (White et al., 2000a,b, 2001), Canada; the Mannville Group of Alberta, Canada; the Boulder Creek Formation of British Colombia, Canada (Ufnar et al., 2001); the Paddy Member of the Peace River Formation of Alberta, Canada (Ufnar et al., 2005); and the Nanushuk Formation of Alaska, U.S.A. (Ufnar et al., 2004c) (Fig. 1). Pedogenic calcites were sampled from the Cedar Mountain Formation of Utah, U.S A., and were presented by Ludvigson et al. (2003). Ludvigson et al. (2004) presented data from paleosols and exposure surfaces of the Antlers Formation of Oklahoma, U.S.A., and the Glen Rose and Walnut Formations of Texas, U.S.A. Suarez et al. (2009) reported isotopic data from exposure surfaces and paleosols from the Tlayua Formation in Puebla, Mexico. Equatorial data comes from sphaerosiderite-bearing paleosols from coastal wetland deposits of the Caballos Formation in the Upper Magdalena Valley of Colombia, and provides our only southern hemisphere locality (Suarez et al., 2010).

2.2. Model description

The original model of Ufnar et al. (2002) attempted to recreate the precipitation and evaporation fluxes that result in simulated sphaerosiderite $\delta^{18}O$ values that match the values of analyzed sphaerosiderites. The mass balance model tracks the evolution of an air mass oxygen isotopic composition and that of resultant precipitation as it travels from equator to pole. The air mass is prescribed an initial isotopic composition (see model calibration below) and at each model step (latitude), the isotopic composition of the vapor changes based on the composition of the water leaving the air mass through precipitation and the composition of the vapor replenishing the air mass through evaporation (Fig. 2). The following equation is used to calculate the isotopic composition of the water vapor in the air mass:

$$\delta^{18}O_{a(n)} = \frac{\delta^{18}O_{a(n-1)} + \left[\left(d_v - \delta^{18}O_{a(n)}\right) * \frac{de}{dt}\right] - \left[\left(d_r - \delta^{18}O_{a(n)}\right) * \frac{dr}{dt}\right]}{f_{(n-1)} + \frac{de}{dt} - \frac{dr}{dt}} \quad (1)$$

Where, $\delta^{18}O_{a(n)}$ = the composition of water vapor in the air mass at a given step in the model,

f	the fraction of vapor remaining in the vapor reservoir,
δ_v	the composition of the vapor added by evaporation,
de/dt	the vapor fraction added to the reservoir by evaporation,
δ_r	the composition of precipitation removed from the air mass, and
dr/dt	vapor fraction removed from the reservoir by precipitation.

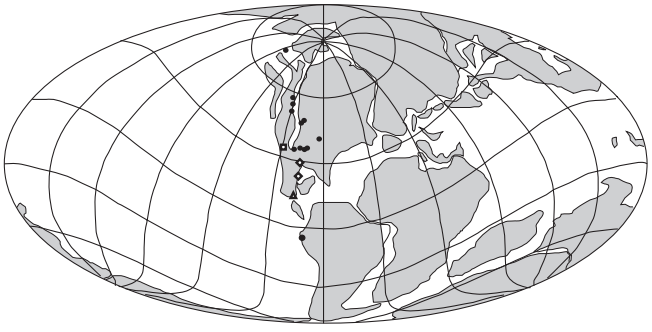

Fig. 1. Global paleogeographic reconstruction for the mid-Cretaceous (105 Ma) showing the distribution of carbonate data localities. Sphaerosiderite-bearing localities are marked by solid symbols. Calcite-bearing localities are marked by open symbols. Paleogeographic reconstruction based on reconstructions by Schettino and Scotese (2004).

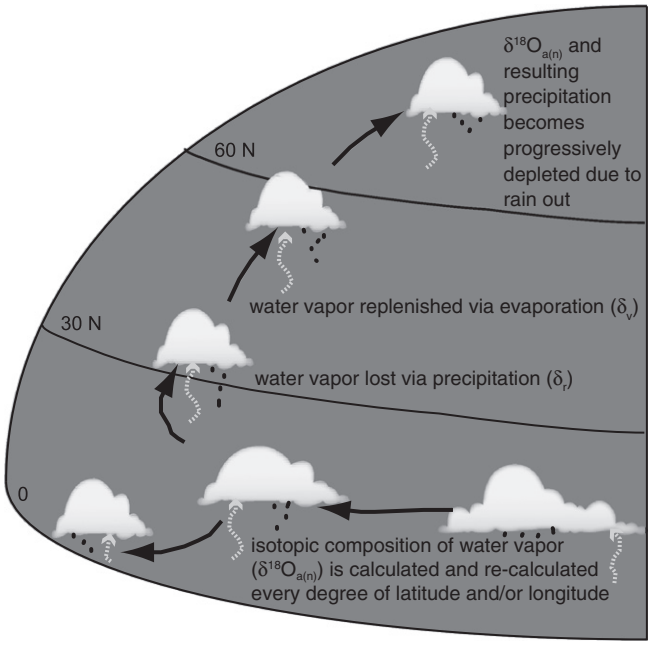

Fig. 2. Conceptual illustration of the mass balance model. As the model progresses for each step the oxygen isotopic composition of water vapor is calculated based on inputs defined by the user that change latitudinally. Precipitation removes water from the air mass and evaporation replenishes it. To simplify the model precipitation and evaporation are set as dimensionless fluxes. The oxygen isotopic composition of water vapor is determined by the depletion due to precipitation and the composition of water replenishing the air mass through evaporation. See also Eq. (1) in text.

The composition of the vapor (δ_v) replenishing the air mass is dependent on the fractionation factor between water and vapor (Majoube, 1971), the composition of the water being evaporated, the evaporation flux (de/dt), and relative humidity. The composition of the precipitation (δr) that depletes the air mass is dependent on the composition of the water vapor in the air mass, the precipitation flux (dr/dt), and the fractionation factor between vapor and water (Majoube 1971).

The revised model also uses Stella® System Modeling software (version 9), but a number of modifications were made. Like the original model, precipitation and evaporation fluxes along with relative humidity are inputs that change based on latitude. The new model iteration also allows for latitudinal changes in the oxygen isotopic composition of seawater, and for changes in the fraction of continental freshwater feedback (treated as a single source that includes evapotranspiration, and evaporation from freshwater bodies and soil water). Latitudinally variable $\delta^{18}O$ of seawater, rather than a constant −1.2‰ VSMOW, is consistent with geologic data that suggest evaporative conditions in the tropics (Woo et al., 1992; Johnson et al., 1996) and high freshwater input at northerly reaches of the Western Interior Seaway (Hay and DeConto, 1999; Poulsen et al., 1999; Huber et al., 2002). In the original modeling, continental freshwater feedback was used in a scenario that maintained a

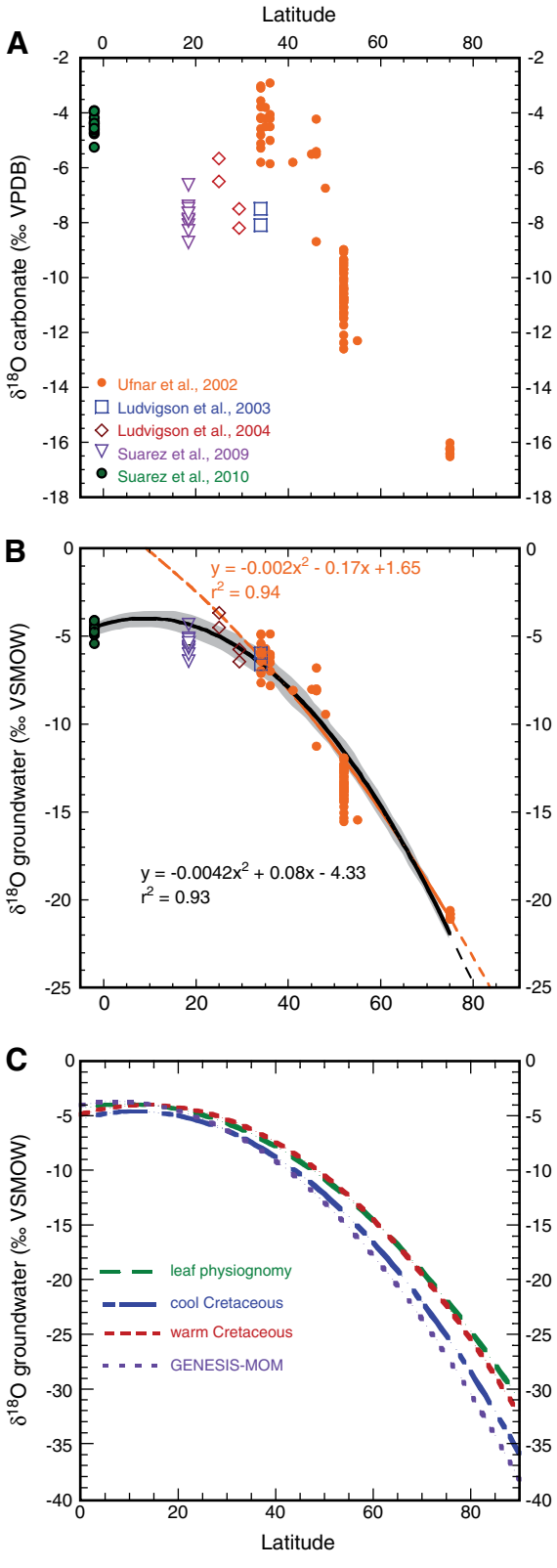

Fig. 3. $\delta^{18}O$ of carbonate and groundwater data utilized in the mass balance model. A) Latitudinal distribution of carbonate data. Calcite data is shown as open symbols and sphaerosiderite data is shown as closed symbols. B) $\delta^{18}O$ of groundwater latitudinal gradient derived from carbonate data in (A) using temperature dependent fractionation factors for calcite from water and siderite from water (Friedman and O'Neil, 1977; Carothers et al., 1988). Temperature was determined based on leaf physiognomy data from Wolfe and Upchurch (1987) and compiled by Spicer and Corfield (1992). The orange line and equation is fit to data of Ufnar et al. (2002). The black line and equation is fit to all data included in this study. Shaded region encompasses 2nd order polynomials fit to the 1σ standard deviations of the $\delta^{18}O$ of water calculated from siderite and calcite $\delta^{18}O$. Dashed parts of the curves are projections of the fit to the data. C) $\delta^{18}O$ of groundwater using 3 additional temperature estimates for the Cretaceous and carbonate $\delta^{18}O$ from analyzed pedogenic calcites and siderites in (A). Cool Cretaceous and warm Cretaceous gradients use temperature estimates of Barron (1983) and the GENESIS-MOM temperature estimates are from GCM outputs provided by Zhou et al. (2008).

Table 1
Temperature gradients and corresponding groundwater gradients utilized in the mass balance model.

	Temperature[a]	$\delta^{18}O$ groundwater[b]
Modern Rozanski et al., 1993	$=-0.003*lat^2-0.2514*lat+30.113$	$=-0.003*lat^2+0.0595*lat-3.699$
Leaf physiognomy Wolfe and Upchurch, 1987; Spicer and Corfield, 1992	$=-0.0006*lat^2-0.2025*lat+30.25$	$=-0.004*lat^2+0.0796*lat-4.329$
Cool Cretaceous Barron (1983)	$=-0.004*lat^2-0.0586*lat+25.662$	$=-0.005*lat^2+0.1137*lat-5.270$
Warm Cretaceous Barron (1983)	$=-0.003*lat^2+0.0538*lat+28.534$	$=-0.005*lat^2+0.1299*lat-4.901$
GENESIS-MOM Zhou et al. (2008)	$=-0.003*lat^2-0.0321*lat+32.514$	$=-0.005*lat^2+0.0730*lat-4.001$

[a] Equation is a second order polynomial fit to data from each reference.
[b] Equation is a second order polynomial fit to groundwater compositions calculated from the $\delta^{18}O$ of carbonate and the temperature at the paleolatitude in which the carbonate was collected. Groundwater values are calculated using the temperature dependent fractionation factors from Friedman and O'Neil (1977) for calcite and Carothers et al. (1988) for siderite.

constant 40% feedback over the entire latitudinal range, regardless of the presence of landmass. This revised model allows for user defined variations over the full latitudinal range.

By including subtropical data from calcites, (Fig. 3A) a different means of matching modeled data to empirical data was needed. To do this the oxygen isotopic composition of waters (presented relative to Standard Mean Ocean Water) that precipitated the pedogenic carbonates were calculated using the respective temperature-dependant fractionation factors (Friedman and O'Neil, 1977 for calcite and Carothers et al., 1988 for siderite), estimated Cretaceous temperatures, and the $\delta^{18}O$ from the analyzed pedogenic carbonates (Fig. 3B). As in Ufnar et al. (2002) the model functionality was initially tested by simulation of a modern data set. While Ufnar et al. (2002) utilized theoretical sphaerosiderite $\delta^{18}O$ compositions derived from precipitation $\delta^{18}O$ values reported in Rozanski et al. (1993), this study uses the latitudinal precipitation $\delta^{18}O$ gradient directly from the same study for the model calibration (Table 1, Model Calibration section below).

We tested four hypothesized temperatures for the Cretaceous (Barron, 1983; Wolfe and Upchurch, 1987; Spicer and Corfield, 1992; Zhou et al., 2008). These temperature gradients were used in combination with the calcite and siderite temperature-dependant fractionation factors to determine four different latitudinal gradients for the oxygen isotopic composition of groundwater (Table 1, Fig. 3C). The $\delta^{18}O$ composition of groundwater approximates the composition of precipitation (Lohmann, 1988) and, thus, the goal is to match the modeled rain compositions with the groundwater compositions calculated from siderites and calcites. In addition, the mean oxygen isotopic compositions of groundwater are used as the compositions of water fed back from the continents. If we extrapolate to the equator using the regression presented by Ufnar et al. (2002) for the compiled latitudinal sphaerosiderite data, a much heavier tropical oxygen isotopic composition is calculated than that obtained from the empirical data presented by Ludvigson et al. (2004) and Suarez et al. (2009, 2010). It is evident that low latitude data are necessary to better constrain our model (Fig. 3).

A significant modification in the new model is the addition of a westward travel path along the subtropical region. This westward travel path is more realistic than a strict equator to pole trajectory because it accounts for the westward airflow that characterizes the trade winds. The model allows the user to select the latitude along which the air mass travels westward as well as the distance traveled by the air mass before it flows north toward the pole or south toward the equator.

3. Model calibration

The model was first calibrated to match precipitation $\delta^{18}O$ compositions with those reported from International Atomic Energy Agency/World Meteorological Organization (IAEA/WMO) stations (Rozanski et al., 1993). These data were filtered to include only coastal stations less than 300 m in elevation to eliminate significant altitude and continental effects. This is consistent with the hypothesized depositional settings of the Cretaceous pedogenic data. The temperature gradient used in the modern model was also derived from Rozanski et al. (1993). The model was started at 10°N latitude and the air mass was tracked west for 50° before deflecting north or south. This distance was chosen because it is approximates the longitudinal distance that modern storm tracks take as they originate off the coast of Africa. The initial isotopic composition of the water vapor in the air mass was set at −10.50‰ VSMOW which is based on observational data presented in Craig and Gordon (1965) for mast height vapor compositions (Table 2). The $\delta^{18}O$ of seawater was defined based on a global gridded data set presented in LeGrande and Schmidt (2006). Latitudinal relative humidity variations were set according to inputs of the original Ufnar et al. (2002) model and adjusted where necessary. For example, in areas where model precipitation was too enriched relative to empirical data, decreasing relative humidity makes precipitation $\delta^{18}O$ lighter due to a greater kinetic effect. Peak continental feedback was set to reflect the peak percentage of land mass distribution at approximately 60°N (Barron et al., 1989). The peak continental feedback was kept low (19%) because we attempt to simulate coastal rain compositions, and it has been suggested that continental feedback affects the oxygen isotopic compositions of precipitation to a greater extent much farther inland (Nijitchoua, 1999).

The primary adjustments for the model to match the observed precipitation compositions were those made to precipitation and evaporation fluxes. Precipitation flux variations attempted to simulate the modern precipitation distributions with a high in the tropics, a low in the subtropics, a secondary peak in precipitation in the mid-latitudes, and low precipitation in the polar regions. The peak precipitation flux for the model occurs at 6°N latitude, where observational data of Alder et al. (2003) indicate peak precipitation rate occurs. Likewise, the distribution of evaporation fluxes attempted to reflect estimated evaporation rates in which evaporation is high in the tropics with a peak between approximately 20° and 30° and then a significant decline poleward. In attempting to match the observed rain composition data, it was necessary to increase the evaporation flux over that of the precipitation flux between 0 and 10°N. This is a reasonable modification because despite high amounts of precipitation in the tropics, high amounts of evaporation are necessary to sustain the water vapor in the air mass. Using these parameters, the model was able to reproduce

Table 2
Initial isotopic compositions of water vapor.

Temperature gradient	$\delta^{18}O_v =$
Modern	−10.50‰
Leaf physiognomy	−10.53‰
Cool Cretaceous	−10.84‰
Warm Cretaceous	−10.60‰
GENESIS-MOM	−10.39‰

observed precipitation compositions within ±0.5‰ VSMOW between 4°N and 90°N and within −0.6‰ VSMOW between 0 and 3°N The model produces rain compositions slightly too light between these latitudes. The input parameters used to reproduce the observed $\delta^{18}O$ of modern precipitation are graphed and summarized in Fig. 4.

4. Model results

After testing model functionality using the modern oxygen isotopic compositions of precipitation, a variety of model scenarios were run using four different Cretaceous latitudinal temperature

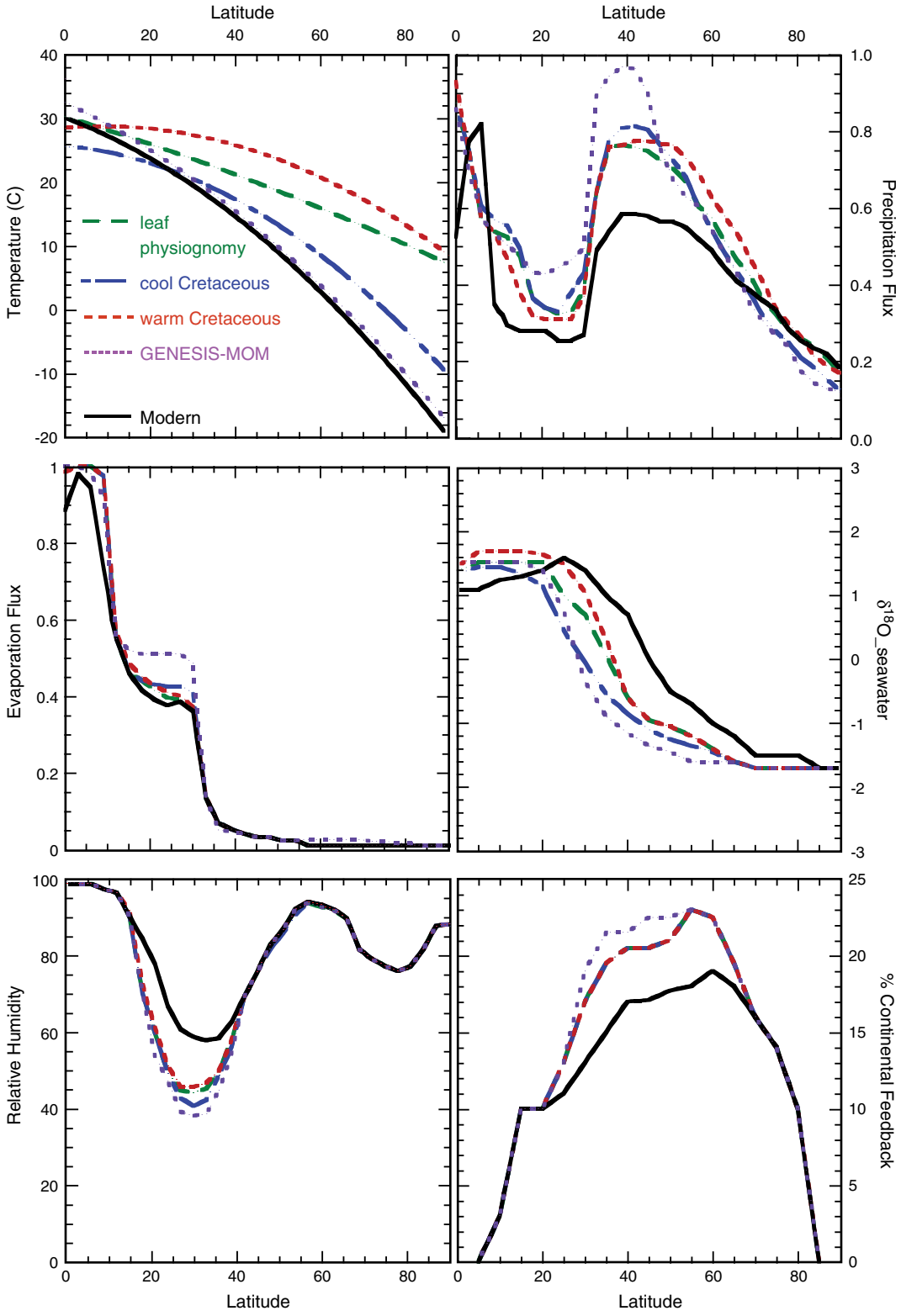

Fig. 4. Inputs for each temperature scenario in the mass balance model that produced precipitation compositions that closely match empirically derived compositions. Temperature scenarios include: modern, warm and cool Cretaceous, leaf physiognomy, and GENESIS-MOM, see text for references for each temperature gradient.

gradients (Table 1). A Cretaceous temperature gradient based on leaf physiognomy data of Wolfe and Upchurch (1987) and Spicer and Corfield (1992) has been used in previous data presented by our research group (Suarez et al., 2009, 2010). We favor this temperature gradient because it is based on interpretations of paleoclimate proxy data rather than modeled data, and it is representative of a terrestrial-based temperature proxy as opposed to marine. The model was also run with warm and cool Cretaceous temperature gradients presented by Barron (1983), and a temperature gradient fit to recent model outputs from the coupled ocean–atmosphere GCM, GENESIS-MOM, for near surface temperatures at 8 times modern atmospheric CO_2 concentrations provided by Zhou et al., 2008.

Air masses in the Cretaceous models started at 5°N rather than 10°N because it has been suggested that the seasonal migration of the Cretaceous inter-tropical convergence zone (ITCZ) was in a more southerly position than the modern ITCZ (Hay and DeConto, 1999). The modeled air mass was tracked west for 50° before it deflected either to the north or south. The initial $\delta^{18}O$ of the water vapor in the air mass (Table 2) for each temperature gradient model was calculated based on an average seawater composition of −1.2‰ VSMOW (Poulsen et al., 2007), the temperature at 5°N (for each temperature gradient), and kinetic effects due to relative humidity (Gonfiantini, 1986; Clark and Fritz, 1997):

$$\delta^{18}O_v = \delta^{18}O_l - (\alpha_{l-v} - 1)*1000 - 14.2*(1-h) \quad (2)$$

where

$\delta^{18}O_v$ the oxygen isotopic composition of water vapor,
$\delta^{18}O_l$ the oxygen isotopic composition of evaporating water,
α_{l-v} the fractionation factor for water from vapor (Majoube, 1971), and
h humidity, which in this case is set at 98% (0.98).

While the average oxygen isotopic composition of sea water for the ice-free mid-Cretaceous has been estimated to be −1.2‰ (Poulsen et al., 2007) which is used to calculate the initial vapor composition, Woo et al. (1992) suggested that the salinity and oxygen isotopic composition of surface seawater was elevated in what is now the Gulf of Mexico, as a result, enriched $\delta^{18}O$ values were assigned for low latitude seawater composition. Using the most enriched $\delta^{18}O$ values of calcite presented by Woo et al. (1992), the heaviest $\delta^{18}O$ values of seawater were calculated as high as 2‰ (VSMOW). Roche et al. (2006) use a coupled ocean–atmosphere model to produce a more conservative maximum $\delta^{18}O$ of seawater of about 1‰ (VSMOW). This is contradicted however, by Zhou et al. (2008) (see Discussion below). In the northern hemisphere where freshwater runoff was high, seawater could have been depleted to as low as −4‰ to −5‰ VSMOW (Woo et al., 1992; Hay and Deconto, 1999; Poulsen et al., 1999; Huber et al., 2002; Zhou et al., 2008).

Using the above constraints, the model inputs (precipitation and evaporation flux, relative humidity, terrestrial feedback, and $\delta^{18}O$ seawater) were adjusted to produce modeled rain compositions that were within ±0.5‰ VSMOW of empirically-derived Cretaceous groundwater compositions for each temperature scenario (Figs. 4 and 5). Precipitation fluxes for the simulations of Cretaceous temperature gradients are generally greater than the modern precipitation flux, with the exception of (1) a small area between 3 and 8°N, and (2) latitudes north of about 70°, especially for the cool Cretaceous and GENESIS-MOM temperature scenarios. Evaporation fluxes are also greater primarily between the equator and 10°N and between 15°N and 30°N. Because our carbonates were obtained from low elevation fluvial systems, evaporative feedback from the landmass to the air mass must be considered.

For all scenarios, the $\delta^{18}O$ of seawater was enriched in the low latitudes (1.45‰ to 1.52‰) and depleted in the high latitudes (−2.00‰ to −1.70‰). The warm Cretaceous scenario requires the most enriched compositions in the equatorial to sub-tropical latitudes. The GENESIS-MOM scenario requires the most depleted values in the mid-latitudes.

Relative humidity must be significantly decreased between 20°N and 40°N. This was required because the model would otherwise produce precipitation $\delta^{18}O$ values that are too enriched relative to the empirically derived precipitation compositions, requiring high precipitation rates to deplete the air mass compositions. However, the sedimentologic evidence (pedogenic calcites and evaporites) indicates precipitation deficits and reduced precipitation rates (Ludvigson et al., 2003; Ludvigson et al., 2004; Suarez et al., 2009). Reducing relative humidity causes a greater kinetic effect on the $\delta^{18}O$ of atmospheric moisture during evaporation, resulting in depletion of the oxygen isotopic composition of subtropical rainwater.

5. Sensitivity and alternate scenarios

A number of sensitivity tests were presented in the original model iterations by Ufnar et al. (2002). In the sensitivity analysis, changes to the seawater composition, continental water composition, relative humidity, evaporation flux, and precipitation flux were made to determine the relative impact of each of these variables on model results. These tests indicated that the model is primarily sensitive to changes in precipitation and evaporation flux. The model is also somewhat sensitive to changes in the isotopic composition of continental water as well as relative humidity.

Sensitivity of the revised model to seawater composition is re-evaluated because unlike the previous model, the seawater composition is changed to reflect hypothesized compositions of seawater (Woo et al., 1992; Johnson et al., 1996; Poulsen et al., 1999; Huber et al., 2002; Zhou et al., 2008). For these sensitivity tests, the model scenario tuned using the leaf physiognomy temperature gradient was changed to reflect (1) a constant seawater $\delta^{18}O$ composition of −1.2‰ VSMOW, (2) a constant heavy tropical seawater $\delta^{18}O$ composition of 1.4‰ VSMOW with a constant light Western Interior Seaway (WIS) $\delta^{18}O$ value of −1.2‰ VSMOW, and (3) $\delta^{18}O$ of surface seawater determined by GENESIS-MOM (Zhou et al., 2008), which is about −1.1‰ at the equator, increases to about 0.9‰ at 25°N and then decreases to −5.7‰ at the pole (Table 3). A constant −1.2‰ VSMOW of seawater, as well as the $\delta^{18}O$ of seawater determined by GENESIS-MOM causes precipitation to become lighter over the full range of latitudes, but especially in the low latitudes. A heavy tropical composition with a constant light Western Interior Seaway has little effect, and precipitation compositions remain within ±0.5‰ of the derived empirical data. Changes to the model that are required to simulate the derived empirical data with the changes made to seawater compositions are shown in Fig. 6. To balance the scenario with a constant −1.2‰ VSMOW seawater composition (and also with the GENESIS-MOM seawater compositions), precipitation flux must be decreased between 0 and 12°N, and increased significantly north of 12° to values that are inconsistent with geologic and paleontologic data (Ludvigson et al., 2003; Ludvigson et al., 2004; Suarez et al., 2009).

A zero continental feedback scenario was run to test the impact of the continental feedback on the isotopic composition of precipitation. Eliminating continental feedback has a very minor effect on the $\delta^{18}O$ of precipitation. The lack of continental feedback causes a maximum 0.8‰ enrichment, which requires a slight increase in precipitation flux to match the empirical data (Fig. 6).

A significant change to the revised model is the addition of westward vapor transport in the tropics, which is somewhat more realistic than a strictly equator-to-pole track that was presented in Ufnar et al. (2002). For the tuned leaf physiognomy scenario, the air mass traveled westward for 50° before diverting north or south as in the modern simulation. Changing the westward travel distance has

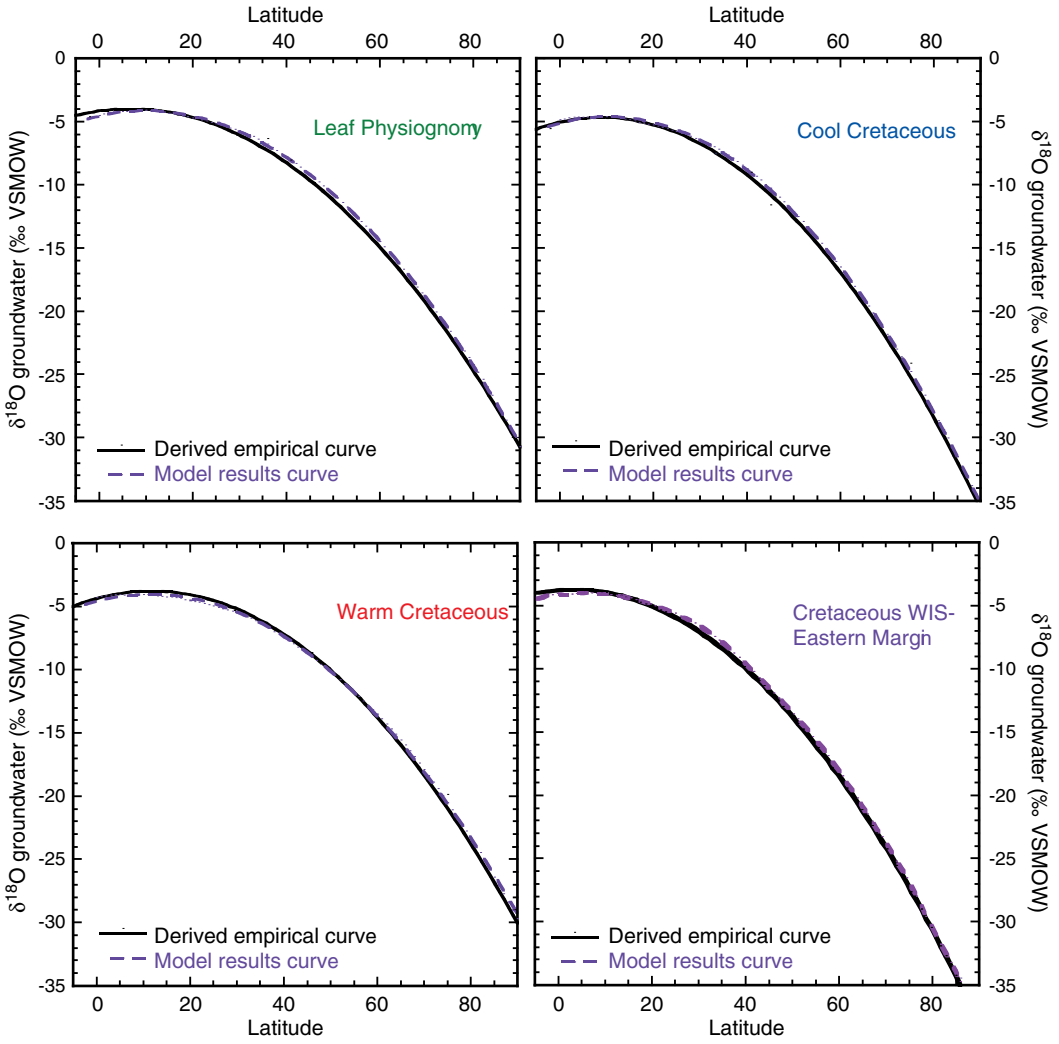

Fig. 5. Empirically-derived $\delta^{18}O$ of groundwater gradients for four different latitudinal temperature gradients scenarios compared with model-produced precipitation compositions (dashed-lines).

significant effects on modeled rain compositions and elucidated two aspects of the model which were previously not recognized.

With longer longitudinal travel distance (example: 70°), the resulting precipitation $\delta^{18}O$ is more enriched at higher latitudes, and with a shorter westward travel distance (10°) or only a simple equator-to-pole transect, the precipitation $\delta^{18}O$ becomes extremely depleted at higher latitudes (Fig. 6). The reason for the enriched precipitation values associated with longer westward travel is partially because the air mass evolves over a source of enriched water for a longer period of time. More significant however, is that the vapor reservoir gains a significant amount of vapor due to a high evaporation flux, such that the reservoir which was initially set at 1, becomes larger than 1 with a longer westward travel path. As a result, the amount of water vapor in the reservoir is exhausted with a short westward travel distance and becomes volumetrically and isotopically depleted before the air mass reaches the pole. The model in its current form does not have a means of limiting the size of the reservoir.

Another effect of the westward air mass track is to stabilize the oxygen isotopic composition of precipitation. During the model run spin-up, the initial air mass and precipitation compositions become lighter, and as the run progresses the $\delta^{18}O$ values become more stable ($\delta^{18}O$ of the air mass stabilizes at approximately −13.2‰). With a strict equator-to-pole transect, the precipitation composition fails to stabilize before becoming too depleted. This initial depletion in the tropics is common to all of the Ufnar et al. (2002) simulations, in which the oxygen isotopic compositions of siderite have a short, but steep depletion between 0 and 10°N before becoming more stable; however, this was un-recognized because the model-proxy comparison in Ufnar et al. (2002) was focused on the mid to high latitudes.

Lastly, we tested the initial vapor compositions by enriching the initial vapor to −7.799‰ (the composition of vapor evaporating from a water body of about 1.5‰), and by depleting the initial vapor to −13.534‰ (slightly lighter than the stabilized vapor composition). While these changes are 3.5 to 4‰ different than the initial vapor set in the tuned leaf physiognomy model, the resulting precipitation compositions do not change, suggesting that the other variables, particularly precipitation and evaporation, are the main drivers of the vapor composition.

6. Precipitation rates

To provide more useful estimates for comparisons, Ufnar et al. (2002) calculated precipitation rates. To do this temperature-dependent

Table 3
Sensitivity tests.

Variable	Tuned leaf physiognomy scenario[a]	Adjustments	Result
Seawater $\delta^{18}O$ (SMOW)	1.4‰ at the equator and increases to 1.52‰ from 5°N to 20°N before steadily decreasing to −1.7‰ at 70°N.	1. Constant 1.4‰ from equator to 25°N and constant −1.2‰ north of 25° 2. constant −1.2‰ 3. surface seawater $\delta^{18}O$ from GENESIS-MOM (Zhou et al., 2008); −1.1‰ at the equator, increases to −0.9‰ at 25°N, decreases to −5.7‰ at 90°N	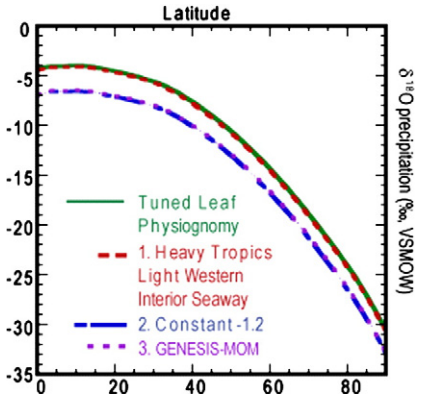
Continental feedback	0% continental feedback between the equator and 5°N and increases to 23% at 55°N before decreasing to 0% at 85°N.	No continental feedback	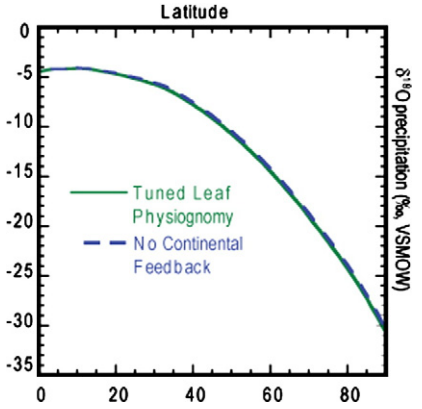
Air mass travel path	Air mass travels westward for 50° before moving north or south	1. air mass travels westward 70° before moving north or south. 2. air mass travels 10° before moving north or south. 3. air mass travels equator to pole.	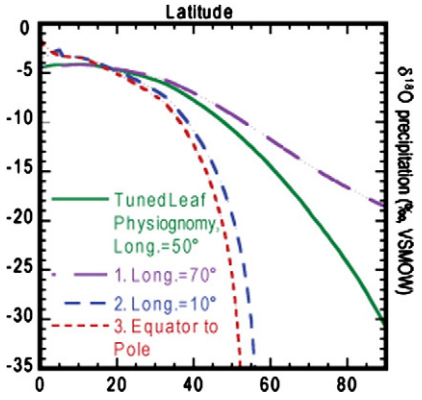
Initial vapor $\delta^{18}O$ (SMOW)	−10.534‰	1. Initial vapor changed to −7.799‰. 2. Initial vapor changed to −13.534‰.	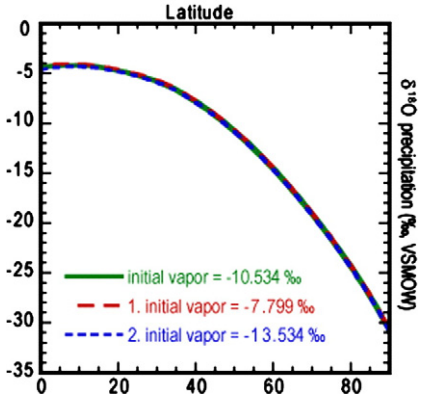

[a] See also Fig. 4.

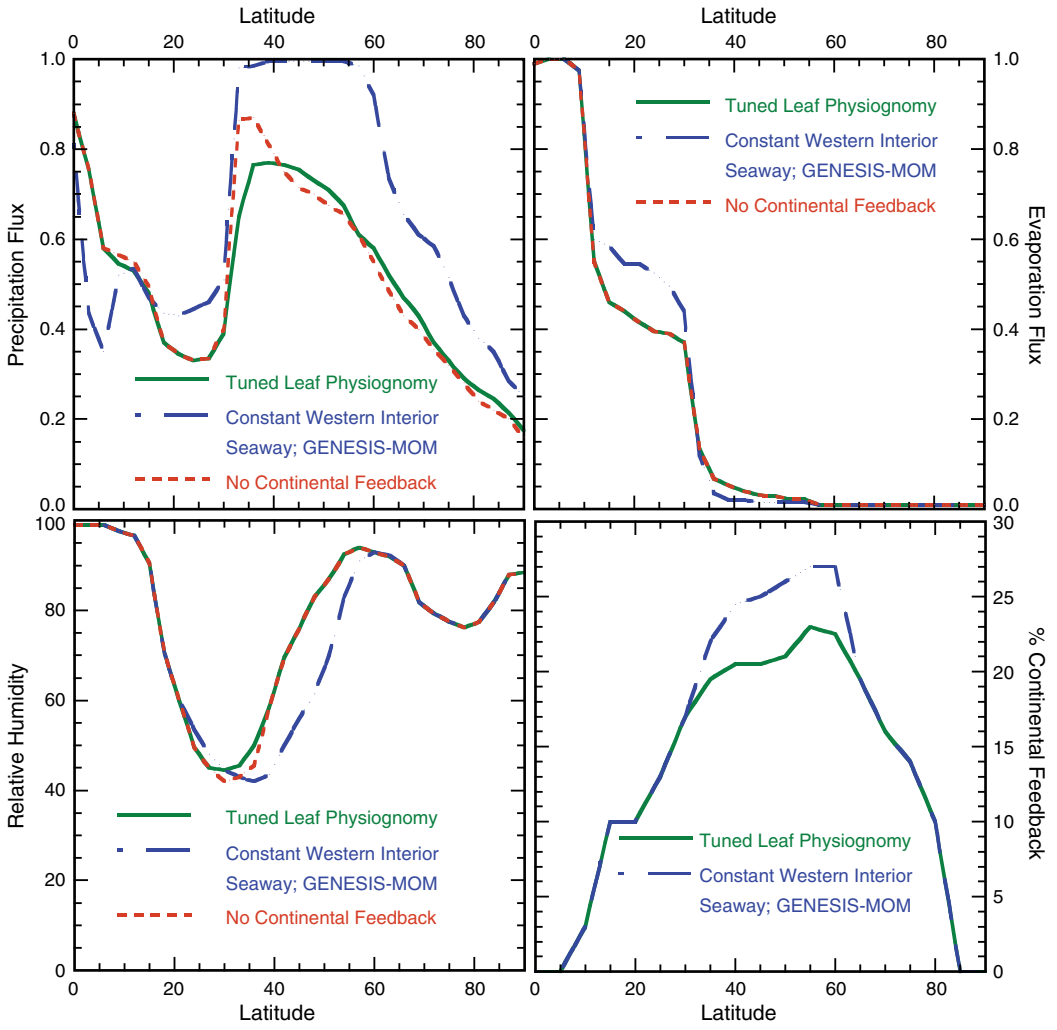

Fig. 6. Input parameters necessary to produce modeled precipitation compositions for alternative scenarios including a constant −1.2‰ VSMOW seawater composition, seawater composition determined by GENESIS-MOM output (Zhou et al., 2008), and no continental feedback.

saturation vapor density curves (Clark and Fritz, 1997) are first used to determine the potential change in saturation vapor density at each latitude between the Cretaceous and modern temperature gradients:

$$VD = 0.002^{*}T^{3} + 0.0111^{*}T^{2} + 0.321^{*}T + 4.8$$
$$\Delta VD_{k-m} = (VD_k - VD_m)/(VD_m) \quad (3)$$

where VD = saturation vapor density (g/m^3), T = temperature in degrees Celsius, and subscripts m refers to modern and k to Cretaceous. It is then assumed that the fractional change in vapor density due to temperature change is proportional to the change in amount of precipitation. We equate the change in precipitation to be encompassed in the height (H) of an infinitesimally small water column (one dimension) over a single spot or latitude. By assuming our fluxes used in the mass balance model are yearly fluxes we can then algebraically solve for Cretaceous precipitation (P_k) rates using the following equations:

$$H_m = P_m / F_m \quad (4)$$
$$H_k = (1 + \Delta VD_{k-m})^{*}H_m$$
$$P_k = H_k{}^{*}F_k$$
$$P_k = (1 + \Delta VD_{k-m})^{*}(P_m / F_m)^{*}F_k$$

where P = precipitation rate, F = precipitation flux, H = height of an infinitesimally small water column, and ΔVD is the change in potential vapor density (defined in equation set 3, above). Modern zonal mean average precipitation rates (P_m) are from combined rain gauge and satellite data between 1979 and 2003 presented by Alder et al. (2003).

The precipitation rates (Fig. 7) calculated for each of the Cretaceous temperature gradient scenarios are greater than modern precipitation rates with the exception of a narrow range between 2°N and 8°N. In addition, north of 69°N the precipitation rate calculated using the GENESIS-MOM temperature gradient scenario, is slightly lower than the modern precipitation rate. For all but the warm Cretaceous temperature gradient (Barron, 1983) scenario, the peak precipitation occurs at 9°N. In the warm Cretaceous scenario maximum precipitation is manifested as a broad peak with a maximum of 3268 mm/year at 59°N. The lowest precipitation rates occur in the subtropics at 20°N to 21°N, however, these rates are still greater than the modern precipitation rates. Peaks in precipitation (at the equator, at 9°N, and between about 45°N and 60°N) vary significantly between the four temperature gradient scenarios. For example, at 55°N, the GENESIS-MOM temperature gradient scenario yields an estimated precipitation rate of 1066 mm/year, the cool Cretaceous scenario of Barron (1983) yields an estimated precipitation rate of 1496 mm/year, the leaf physiognomy scenario yields an estimated precipitation rate of 2146 mm/year, and the warm Cretaceous scenario of Barron (1983) yields an estimated precipitation rate of 3167 mm/year. The total range in estimated precipitation rates at this latitude is 2101 mm/year.

The precipitation rate estimates of this revised model are lower than the estimates of Ufnar et al. (2002). For example, at 45°N, the leaf physiognomy temperature gradient of the original model produced a precipitation rate of 2618 mm/year, whereas the revised model indicates a precipitation rate of 1922 mm/year. Precipitation rates for the other temperature gradient scenarios are also lower. Recently, Poulsen et al. (2007) generated precipitation rates and oxygen isotopic compositions using the GENESIS atmospheric general circulation model (GCM) for various CO_2 concentrations. Precipitation rates increased with increased CO_2 concentrations. The lowest (2 time modern CO_2) and highest (12 times modern CO_2) precipitation rate curves for these model simulations are also depicted in Fig. 7. The GENESIS precipitation rate patterns are somewhat different than those produced by the mass balance model. The GCM precipitation rates are symmetrical about the equator with peak precipitation at the equator. Like the mass balance model results, the low in precipitation rates occurs at approximately 20°N to 21°N and a secondary peak in precipitation occurs in the mid-latitudes. Global precipitation rates for the mass balance models and for the GCM simulations of 2 and 12 time modern CO_2 concentrations are summarized in Table 4. The leaf physiognomy scenario and warm Cretaceous (Barron, 1983) scenario suggest precipitation rates that are greater than the extreme 12 times CO_2 simulation. The cool Cretaceous scenario is less than the least extreme (2 times CO_2) model output. The GENESIS-MOM scenario produces global precipitation rates that are slightly less than the 2 times CO_2 simulation, but still greater than the cool Cretaceous scenario.

10. Discussion

The mass balance model presented here, while not as complex as a GCM, provides important insights into the variables that need to be considered for improving modeling of the hydrologic cycle. An obvious variable that receives attention in climate models is that of temperature. The different temperature gradients utilized in the mass balance models result in very different precipitation rates, suggesting that current uncertainties concerning Cretaceous temperatures must be reconciled in order to improve precipitation estimates. Recent advances in temperature proxies such as clumped isotope methods (Ghosh et al., 2006; Eiler, 2007) and utilization of organic molecules (Schouten et al., 2003) may in the future provide better constrained paleotemperature gradients.

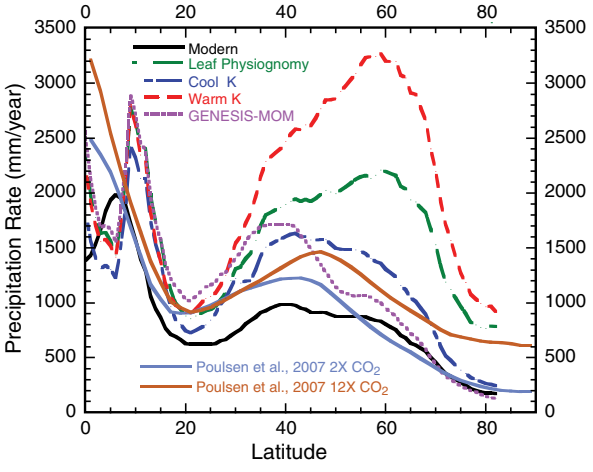

Fig. 7. Annual precipitation rates calculated for each temperature gradient scenario. Light blue and orange solid lines are precipitation rates produced by GENESIS GCM simulations based on 2*x* modern CO_2 concentrations and 12*x* modern CO_2 concentrations. These rates are based on data presented in Poulsen et al. (2007).

Table 4
Average global precipitation rates.

	Precipitation rate (mm/year)
Modern (Alder et al., 2003)[a]	851
Leaf physiognomy (this study)[b]	1629
Cool Cretaceous (this study)[b]	1198
Warm Cretaceous (this study)[b]	2047
GENESIS-MOM (this study)[b]	1228
2x modern CO_2 simulation (Poulsen et al., 2007)[c]	1241
12x modern CO_2 simulation (Poulsen et al., 2007)[c]	1424

[a] Average rate given in Alder et al. (2003).
[b] Average rate for each temperature scenario calculated using equation sets 3 and 4.
[c] Average rate given in Poulsen et al. (2007).

Sensitivity testing indicates that the origin and pathway that air masses travel as well as the size of the water vapor reservoir in the air mass significantly affects $\delta^{18}O$ of precipitation values. In modeling air mass pathways, the mass balance model lacks the sophistication of a general circulation model, which can simulate the complexity of air circulation and cloud dynamics far better than the mass balance model, and may be why significant differences occur in precipitation rates as well as isotopic compositions of precipitation.

A related variable is that of paleogeography and paleotopography. Barron et al. (1989) indicated that the distribution of landmasses plays a significant role ocean circulation, and in the availability of moisture for the atmosphere as well as the distribution of rainfall. In addition, differences in heating of land compared to sea affects air circulation. In the high mountain GENESIS GCM simulation of, Poulsen et al. (2007), topography played a significant role in the oxygen isotopic composition of simulated rainfall in a site bordering the ancestral Brooks Range along the North Slope of Alaska. Precipitation $\delta^{18}O$ modeled by GENESIS in this region is more enriched than our estimates. By increasing topography in this region, however, Poulsen et al. (2007) show that $\delta^{18}O$ of precipitation becomes more depleted and closer to estimates presented in this study due to temperature and amount effects in which the air mass is driven upward by high mountains and cools and condenses driving Rayleigh distillation. Poulsen et al. (2007) argued that these orographic effects caused the local isotopic depletion of sphaerosiderite compositions and not the zonally increased rainout effects on polar paleoprecipitation of the global hydrologic cycle. In first presenting the Alaskan data from the Cretaceous Nanushuk Group, Ufnar et al. (2004a) noted similarities between their estimates of depleted polar Cretaceous paleoprecipitation to those presented by Ferguson et al. (1999) from polar sites of southern Australia suggesting depleted $\delta^{18}O$ is not a local feature specific to the North Slope of Alaska. Phillips et al. (2007) suggested that sphaerosiderites sampled from interfluvial settings of coastal environments were precipitated by more enriched porewaters than early cements in adjacent fluvial environments, and that drainage of higher altitude, and thus depleted precipitation, was responsible for this observation. Dutton et al. (2005), also shows depleted river water $\delta^{18}O$ relative to local precipitation especially in areas of high topography. Because all sphaerosiderites sampled by our research group were precipitated in interfluvial settings of coastal environments we suggest that groundwater responsible for siderite precipitation was dominated by local coastal paleoprecipitation, as opposed to regional fluvial runoff which is influenced by topographic effects. Despite this, topography is an important factor in the distribution of oxygen isotopic composition of precipitation today (Bowen and Wilkinson, 2002), and was likely an important factor in the Cretaceous. There is no doubt that greater spatial sampling resolution of continental oxygen isotopic composition proxies would help elucidate the importance of local topographic or more regional "catchment effects" (Dutton et al., 2005) during the Cretaceous.

Large reduction of relative humidity was necessary for the Cretaceous simulations in the subtropics in order to cause sufficient

depletion without increasing precipitation over evaporation flux. Hay and DeConto (1999) indicated that a contrast in humidity along with overall increased water vapor content could allow for a more efficient poleward latent heat transport during the Cretaceous. Currently there are few methods to estimate humidity in the geologic record. ^{17}O-excess has been used to investigate relative humidity changes recorded in the Vostok ice core, but its utility in the geologic record is still in the early stages of investigation (Landais et al., 2008).

Sensitivity testing presented in Ufnar et al. (2002) as well as those presented here suggest that the oxygen isotopic composition of seawater, particularly in the low latitudes, is an important factor to consider. Numerous authors have recognized that it is unreasonable to model the Cretaceous hydrologic cycle with a constant seawater composition (Woo et al., 1992; Poulsen et al., 1999; Huber et al., 2002). Increased evaporation in the tropics and subtropics caused enrichment of seawater (Woo et al., 1992; Johnson et al., 1996; Poulsen et al., 1999; Ziegler et al., 2003) to δ^{18}O values greater than the average −1.2‰ VSMOW. Conversely, isotopic compositions in the high latitudes were much lighter (as light as −5‰ VSMOW) as result of increased continental runoff, an effect of greater precipitation (Woo et al., 1992; Poulsen et al., 1999; Huber et al., 2002; Zhou et al., 2008). Recent modeling of δ^{18}O of ancient seawater, however, is somewhat ambiguous. For example Roche et al. (2006) suggests increased δ^{18}O of seawater in low latitude surface and intermediate water (approximately 1‰) and decreases in high latitude seawater, especially, high latitude deep water. This is explained by the export of isotopically light water vapor to high latitudes. As mentioned above, Zhou et al. (2008) model fairly light seawater compositions in the low latitudes (maximum of about −0.9‰), and even more significantly depleted seawater poleward. This pattern is explained by the hypothesized formation of saline intermediate to deep water in the subtropical Tethys, which removes enriched seawater, and leaves the low latitude surface waters relatively more depleted.

For the mass balance model, the more enriched isotopic composition of seawater in the tropics to subtropics was an important change because, when modeled with a −1.2‰ VSMOW constant seawater composition, the δ^{18}O of precipitation became too light between 0 and 10°N. The oxygen isotopic composition of seawater is an important target for proxy data sets as seawater δ^{18}O is also important to oxygen isotope paleothermometry. This is another avenue in which clumped-isotope thermometry can prove useful, because not only can this technique provide a temperature estimate; but because δ^{18}O of the carbonate is also analyzed, the δ^{18}O of the precipitating fluid can be calculated.

11. Conclusions

Understanding the dynamics of the hydrologic cycle is an important aspect to providing insight into the global climate system. This revised mass balance model utilizes the oxygen isotopic composition of pedogenic carbonates (calcite and siderite) as a proxy for the oxygen isotopic composition of precipitation, and model inputs (precipitation flux, evaporation flux, seawater composition, relative humidity, and continental feedback) are adjusted to produce modeled oxygen isotopic compositions of modern and mid-Cretaceous precipitation that are within ±0.5‰ VSMOW of derived-empirical data. The various modeling scenarios indicate that temperature (four scenarios were tested), precipitation flux, and evaporation flux are the primary factors that affect the oxygen isotopic composition of precipitation. Our model indicates that Cretaceous evaporation and precipitation was greater than modern evaporation and precipitation over all latitudes with little exception. In addition, relative humidity was significantly decreased in the subtropical dry belts. Using precipitation flux estimates from the model, we calculate precipitation rates that ranged between 371 mm/year and 1196 mm/year greater than modern precipitation rates and provide further support to the hypothesis that the hydrologic cycle was more active during the mid-Cretaceous greenhouse climate. Sensitivity testing indicates that amount of water vapor in an air mass, origin and pathways of air masses, the oxygen isotopic composition of seawater, and humidity are also factors that must be taken into consideration in determining the oxygen isotopic composition of precipitation. Greater constraints for these variables will significantly improve our ability to accurately model ancient and future hydrologic cycles.

Acknowledgements

This study was supported by National Science Foundation grant #EAR-0325072 to González and Ludvigson. We wish to thank Dr. Chris Poulsen and Jing Zhou for sharing GENESIS modeling data for comparison with this study.

References

Alder, R.F., Huffmann, G.J., Chang, A., Ferraro, R., Xie, P., Janowiak, J., Rudolf, B., Schneider, U., Curtis, S., Bolvin, D., Gruber, A., Susskind, J., Arkin, P., Nelkin, E., 2003. The Version 2-Global Precipitation Climatology Project (GPCP) monthly precipitation analysis (1979–present). J. Hydrometeor. 4, 1147–1167.

Allan, J.R., Matthews, R.K., 1977. Carbon and oxygen isotopes as diagenetic and stratigraphic tools: surface and subsurface data, Barbados, West Indies. Geology 5, 16–20.

Barron, E.J., 1983. Warm equable Cretaceous, the nature of the problem. Earth Sci. Rev. 19, 305–338.

Barron, E.J., Hay, W.W., Thompson, S., 1989. The hydrologic cycle: a major variable during earth history. Palaeogeogr. Palaeoclimatol. Palaeoecol. 75, 157–174.

Bowen, G.J., Wilkinson, B., 2002. Spatial distribution of δ^{18}O in meteoric precipitation. Geology 30, 315–318.

Carothers, W.W., Adami, L.H., Rosenbauer, R.J., 1988. Experimental oxygen isotope fractionation between siderite-water and phosphoric acid liberated CO_2-siderite. Geochim. Cosmochim. Acta 52, 2445–2450.

Clark, I., Fritz, P., 1997. Environmental Isotopes in Hydrogeology. Lewis Publishers, New York. 328 pp.

Craig, H., Gordon, L.I., 1965. Deuterium and oxygen 18 variations in the ocean and the marine atmosphere. In: Tongiorgi, E. (Ed.), Stable Isotopes in Oceanographic Studies and Paleotemperatures. Consiglio Nazionale delle Ricerche Labratorio di Geologia Nucleare, Pisa. 125 pp.

Dutton, A., Wilkinson, B.H., Welker, J.M., Bowen, G.J., Lohmann, K.C., 2005. Spatial distribution of seasonal variation in ^{18}O/^{16}O of modern precipitation and river water across the conterminous USA. Hydrol. Processes 19, 4121–4146.

Eiler, J.M., 2007. "Clumped-isotope" geochemistry—the study of naturally-occurring, multiply substituting isotopologues. Earth Planet. Sci. Lett. 262, 309–327.

Ferguson, K.M., Gregory, R.T., Contantine, A., 1999. Lower Cretaceous (Aptian–Albian) secular changes in the oxygen and carbon isotope record from high paleolatitude, fluvial sediments, southeast Australia: comparisons to the marine record. In: Barrera, E., Johnson, C.C. (Eds.), The Evolution of the Cretaceous ocean climate system: Geol. Soc. Am. Spec. Pap., 332, pp. 59–72. Boulder.

Friedman, I., O'Neil, J.R., 1977. Compilation of stable isotope fractionation factors of geochemical interest. In: Fleisher, N. (Ed.), Data of geochemistry: USGS Professional Paper 440-KK: Washington, D.C. . 110 pp.

Ghosh, P., Adkins, J., Affek, H., Balta, B., Guo, W., Schauble, E.A., Schrag, D., Eiler, J.M., 2006. 13C–18O bonds in carbonate minerals: A new kind of paleothermometer. Geochim. Cosmochim. Acta 70, 1439–1456.

Gonfiantini, R., 1986. Environmental isotopes in lake studies. In: Fritz, P., Fontes, J.Ch. (Eds.), Handbook of Environmental Isotope Geochemistry. The Terrestrial Environment, 2. B. Elsevier, Amersterdam, pp. 113–168.

Hay, W.W., DeConto, R.M., 1999. Comparison of modern and Late Cretaceous meridional energy transport and oceanology. In: Barrera, E., Johnson, C.C. (Eds.), The Evolution of the Cretaceous Ocean–Climate system: Geol. Soc. Am. Spec. Pap., 332, pp. 283–300. Boulder.

Huber, B.T., Norris, R.D., MacLeod, K.G., 2002. Deep-sea paleotemperature record of extreme warmth during the Cretaceous. Geology 30, 123–126.

Jenkyns, H.C., Forster, A., Schouten, S., Sinninghe Damste, J.S., 2004. High temperatures in the Late Cretaceous Arctic Ocean. Nature 432, 888–892.

Johnson, C.C., Barron, E.J., Kauffmann, E.G., Arthur, M.A., Fawcett, P.J., Yasuda, M.K., 1996. Middle Cretaceous reef collapse linked to ocean heat transport. Geology 24, 376–380.

Landais, A., Barkan, E., Luz, B., 2008. Record of δ^{18}O and ^{17}-O excess in ice from Vostok Antarctica during the last 150,000 years. Geophys. Res. Lett. 35, L02709.

LeGrande, A.N., Schmidt, G.A., 2006. Global gridded data set of the oxygen isotopic composition in seawater. Geophys. Res. Lett. 33, L12604.

Lohmann, K.C., 1988. Geochemical patterns of meteoric diagenetic systems and their application to studies of paleokarst. In: James, N.P., Choquette, P.W. (Eds.), paleokarst. Springer, New York, pp. 58–80.

Ludvigson, G.A., Ufnar, D.F., González, L.A., Carpenter, S.J., Witzke, B.J., Brenner, R.L., Davis, J., 2004. Terrestrial paleoclimatology of the Mid-Cretaceous greenhouse; I, Cross-calibration of pedogenic siderite & calcite δ^{18}O proxies at the Hadley Cell boundary. Geol. Soc. of Am. 2004 annual meeting: Abstracts with Programs, 36. 305 pp., Boulder.

Ludvigson, G., González, L.A., Metzger, R.A., Witzke, B.J., Brenner, R.L., Murillo, A.P., White, T.S., 1998. Meteoric sphaerosiderite lines and their use for paleohydrology and paleoclimatology. Geology 26, 1039–1042.

Ludvigson, G.A., González, L.A., Kirkland, J.I., Joeckel, R.M., 2003. A mid-Cretaceous record of carbon isotope excursions in palustrine carbonates of the Cedar Mountain Formation of Utah: marine–terrestrial correlations of Aptian–Albian oceanic anoxic events 1a, 1b, and 1d. The Third Internat. Limnogeol. Congress, March 29–April 2, Abstract Volume, Tucson. 169 pp.

Majoube, M., 1971. Fractionment en oxygene-18 et en deuterium entré l'eau at sa vapeur. J. Chim. Phys. 10, 1423–1436.

Nijitchoua, R., 1999. Variations of the stable isotopic compositions of rainfall events from the Cameroon rainforest, Central Africa. J. Hydrol. 223, 17–26.

Phillips Jr., P.L., Ludvigson, G.A., Joeckel, R.M., González, L.A., Brenner, R.L., Witzke, B.J., 2007. Sequence stratigraphic controls on synsedimentary cementation and preservation of dinosaur tracks; example from the Lower Cretaceous, (upper Albian) Dakota Formation, southeastern Nebraska, U.S.A. Palaeogeogr. Palaeoclimatol. Palaeoecol. 246, 367–389.

Poulsen, C.J., Barron, E.J., Peterson, W.H., Wilson, P.A., 1999. A reinterpretation of mid-Cretaceous shallow water temperatures through model-data comparison. Paleoceanography 14, 679–697.

Poulsen, C.J., 2004. A balmy arctic: Nature 432, 814–815.

Poulsen, C.J., Pollard, D., White, T.S., 2007. General circulation model simulation of the $\delta^{18}O$ content of continental precipitation in the middle Cretaceous: a model-proxy comparison. Geology 35, 199–202.

Roche, D.M., Donnadieu, Y., Puceat, E., Paillard, D., 2006. Effect of changes in d18O content of the surface ocean on estimated sea surface temperature in warm past climate. Paleoceanography 21, PA2023.

Rozanski, K., Araguas-Araguas, L., Gonfiantini, R., 1993. Isotopic patterns in modern global precipitation. In: Swart, P.K., Lohmann, K.C., McKenzie, J., Savin, S. (Eds.), Climate Change in Continental Isotope Records: Amer. Geophys. Union, pp. 1–36.

Ruddiman, W.F., 2005. Plow, Plagues, and Petroleum: How humans took control of climate: Princeton. Princeton University Press.

Schettino, A., Scotese, C.R., 2004. Plate Tectonic Reconstructions On-line Paleogeographic Mapper. http://www.serg.unicam.it/Reconstructions.htm.

Schouten, S., Hopmans, E.C., Forster, A., van Bruegal, Y., Kuypers, M.M.M., Sinninghe Damste, J.S., 2003. Extremely high sea surface temperatures at low latitudes during the middle Cretaceous as revealed by archaeal membrane lipids. Geology 31, 1069–1072.

Soreghan, G.S., Maples, C.G., Parrish, J.T., 2003. Report of the NSF sponsored workshop on paleoclimate, in Paleoclimate Workshop. National Science Foundation, Arlington, VA.

Sorensen, A.C., 2002. Petrography and diagenesis of palustrine carbonate beds in the Early Cretaceous Cedar Mountain Formation, eastern Utah. Abstracts with Programs—Geol. Soc. of Am. Boulder, pp. 17–18.

Spicer, R.A., Corfield, R.M., 1992. A review of terrestrial and marine climates in the Cretaceous with implications for modelling the 'Greenhouse Earth'. Geol. Mag. 2, 169–180.

Suarez, M.B., González, L.A., Ludvigson, G.A., Vega, F.J., Alvarado-Ortega, J., 2009. Isotopic composition of low-latitude paleoprecipitation during the Early Cretaceous. Geol. Soc. Am. Bull. 121, 1584–1595.

Suarez, M.B., Gonzalez, L.A., Ludvigson, G.A., 2010. Estimating the oxygen isotopic composition of equatorial precipitation during the mid-Cretaceous. J. Sediment. Res. 80, 480–491.

Ufnar, D.F., González, L.A., Ludvigson, G.A., Brenner, R.L., Witzke, B.J., 2001. Stratigraphic implications of meteoric sphaerosiderite $\delta^{18}O$ values in paleosols in the Cretaceous (Albian) Boulder Creek Formation, NE British Colombia Foothills, Canada. J. Sediment. Res. 71, 1017–1028.

Ufnar, D.F., González, L.A., Ludvigson, G.A., Brenner, R.L., Witzke, B.J., 2002. The mid-Cretaceous water bearer: isotope mass balance quantification of the Albian hydrologic cycle. Palaeogeogr. Palaeoclimatol. Palaeoecol. 188, 51–71.

Ufnar, D.F., González, L.A., Ludvigson, G.A., Brenner, R.L., Witzke, B.J., 2004a. High latitude meteoric $\delta^{18}O$ compositions: Paleosol siderite in middle Cretaceous Nanushuk Formation, North Slope, Alaska. GSA Bulletin 116, 463–473.

Ufnar, D.F., González, L.A., Ludvigson, G.A., Brenner, R.L., Witzke, B.J., 2004b. Evidence for increased latent heat transport during the Cretaceous (Albian) greenhouse warming. Geology 32, 1049–1052.

Ufnar, D.F., González, L.A., Ludvigson, G.A., Brenner, R.L., Witzke, B.J., 2004c. Diagenetic overprinting of the sphaerosiderite paleoclimate proxy: are records of pedogenic groundwater d18O values preserved. Sedimentology 51, 127–144.

Ufnar, D.F., Ludvigson, G.A., González, L.A., Brenner, R.L., Witzke, B.J., Leckie, D.A., 2005. Ancient landscape development in the Late Albian Western Canadian Foreland Basin. J. Sediment. Res. 75, 984–996.

White, T.S., Witzke, B.J., Ludvigson, G.A., 2000a. Evidence for an Albian Hudson arm connection between the Cretaceous Western Interior Seaway. GSA Bulletin 112, 1342–1355.

White, T.S., Witzke, B.J., Ludvigson, G.A., Brenner, R.L., Gonzalez, L.A., Ravn, R.L., 2000b. The paleoclimatological significance of Albian (mid-Cretaceous) sphaerosiderites from eastern Saskatchewan and western Manitoba. Summary of investigation 2000: Saskatchewan Geological Survey, Sask. Energy Mines, misc. rep. 2000–4 1, pp. 63–75.

White, T.S., Gonzalez, L.A., Ludvigson, G.A., Poulsen, C.J., 2001. Middle Cretaceous hydrologic cycle of North America. Geology 29, 363–366.

Wolfe, J.A., Upchurch, G.J.R., 1987. North American nonmarine climates and vegetation during the Late Cretaceous. Palaeogeogr. Palaeoclimatol. Palaeoecol. 61, 31–77.

Woo, K.S., Anderson, T.F., Railsback, L.B., Sandberg, P.A., 1992. Oxygen isotopic evidence for high salinity surface seawater in the mid-Cretaceous Gulf of Mexico: implications for warm, saline deepwater formation. Paleoceanography 7, 673–685.

Zhou, J., Poulsen, C.J., Pollard, D., White, T.S., 2008. Simulation of modern and middle Cretaceous marine $\delta^{18}O$ with an ocean–atmosphere general circulation model. Paleoceanography 23, PA3223.

Ziegler, A.M., Eshel, G., McAllister Rees, P., Rothfus, T.A., Rowley, D.B., Sunderlin, B., 2003. Tracing the tropics across land and sea: Permian to present. Lethia 36, 227–254.